



Quantum first detection of a quantum walker on a perturbed ring

Ya-Jing Wang,¹ Ruo-Yu Yin²,, Ling-Yu Dou,¹ An-Ning Zhang,¹ and Xin-Bing Song^{1,*}

¹*School of Physics, Beijing Institute of Technology, Beijing 100081, China*

²*Department of Physics, Institute of Nanotechnology and Advanced Materials, Bar-Ilan University, Ramat-Gan 52900, Israel*



(Received 17 November 2022; accepted 8 March 2023; published 24 March 2023)

The problem of quantum first detection time has been extensively investigated in recent years. Employing the stroboscopic measurement protocol, we consider such a monitored quantum walk on sequentially or periodically perturbed rings and focus on the statistics of first-detected return time, namely, the time it takes a particle to return to the initial state for the first time. Using time-independent perturbation theory, we obtain the general form of the eigenvalues and eigenvectors of the Hamiltonian. For the case of a sequentially perturbed ring system, we find steplike behaviors of $\sum_{n=1}^{\mathcal{N}} nF_n$ ($\rightarrow \langle n \rangle$ as $\mathcal{N} \rightarrow \infty$) when \mathcal{N} increases, with two plateaus corresponding to integers, where F_n is the first detected return probability at the n th detection attempt. Meanwhile, if the initial condition preserves the reflection symmetry, the mean return time is the same as the unperturbed system. For the periodically perturbed system, similar results can also appear in the case where the symmetry is preserved; however, the size of the ring, the interval between adjacent perturbations, and the initial position may change the mean return time in most cases. In addition, we find that the decay rate of the first detection probability F_n decreases with the increase in perturbation amplitude. More profoundly, the symmetry-preserving setup of the initial conditions leads to the coincidence of F_n . The symmetry of the physical systems under investigation is deeply reflected in the quantum detection time statistics.

DOI: [10.1103/PhysRevResearch.5.013202](https://doi.org/10.1103/PhysRevResearch.5.013202)

I. INTRODUCTION

The classical first-passage problem is one of the most basic issues in statistical mechanics. In the classical random walk, a walker starts at the initial position r_{in} and reaches the target position r_{d} for the first time at a certain time, which is considered to be the first-passage process [1]. The classical first-passage-time problem has been extensively studied, as it has a large number of applications in a variety of scientific fields [2–8]. The quantum extension of this problem is the quantum first-detection problem, and it exhibits some different behaviors compared with the classical first-passage problem.

The time statistics of the quantum first-detection problem has attracted a great deal of theoretical attention [9–29]. Using a periodical monitoring method (see details below), Grünbaum *et al.* [11] proved that a monitored quantum walk on a finite graph can always return to the initial state, i.e., the system is recurrent with the Pólya number as 1 [30], and the expectation of the first return time is an integer times the measurement period. The quantization of the mean first return time has been observed on an IBM quantum computer [31]. In addition, Krovi and co-workers [13–16] showed that the first

hitting time of a quantum walk is sensitively dependent on the initial conditions, and different hitting times could be generated for different initial states. Besides that, the degeneracy of the evolution operator's eigenvalues also has some influence on the hitting time. When the evolution operator is highly degenerate, it is possible to have some initial states that give infinite hitting times, due to which the system is driven into dark states [32]. The degeneracy of the evolution operators arises due to the symmetry of graphs, and the symmetry of graphs is likely to play an important role in the speedups and slowdowns of quantum walks.

As a factor affecting the symmetry of a system, disorder is inevitable in most quantum systems. Quantum walk with disorder has been studied both theoretically and experimentally, and various kinds of interesting dynamical phenomena were demonstrated, such as ballistics and diffusive spreading [33–38] and Anderson and bound-state localization [37–43]. In the tight-binding quantum walk, disorder can be represented by the nonzero on-site energies of a Hamiltonian. When the nonzero on-site energies are small, they are called perturbations. The turning on of disorder results in the removal of degeneracy of a ring Hamiltonian's energy levels, and the time distribution exhibits a slowly decaying tail in a non-Hermitian quantum system [24]. The first return time depends on the effective dimension of the underlying Hilbert space, which is given by the number of distinct energy levels whose overlaps with the target state are nonzero [19]. Therefore the number of the system Hamiltonian's energy levels determines the first return time to a large extent. If the degeneracy of the disordered system's Hamiltonian can be regulated, the first return time can also be regulated. Mülken

*songxinbing@bit.edu.cn

Published by the American Physical Society under the terms of the [Creative Commons Attribution 4.0 International license](https://creativecommons.org/licenses/by/4.0/). Further distribution of this work must maintain attribution to the author(s) and the published article's title, journal citation, and DOI.

et al. [44] showed that the degeneracy of a ring system's Hamiltonian with traps was affected by the spatial distribution of traps, and the spatial distribution of traps also had a significant effect on the mean quantum survival probability. Especially, when traps were periodically arranged on the ring, the mean quantum survival probability decayed asymptotically to a nonzero value, which depends on the ring size and the number of traps. When traps were consecutively arranged on the ring and the number of traps was half of the ring size, the mean quantum survival probability was independent of the ring size, and its decay rate was related to the strength of the traps [44]. Similarly, in classical systems, recently, Pozzoli and De Bruyne [45] studied the survival probability of random walks on a ring with periodically distributed traps and showed the dependence of the decay rate of the survival probability on the trap's length for discrete-time random walks.

The goal of this paper is to investigate the effect of spatial distribution and strength of perturbations on the time statistics of a quantum walk on a ring. We focus on the first detected return time in this paper, namely, the time it takes a monitored quantum walker to return to the initial state for the first time, since the mean of the first detected return time reveals some of the topology of the problem (see below) [11,19]. A previous study has shown that, with a single defect, the mean first return time is still the same as in the clean system, if the initial state does not break the reflection symmetry of the system, and otherwise, the mean first return time increases [21]. Therefore the mean first return time is closely related to the choice of the initial state.

In this paper, we consider two special cases of perturbations' distribution, i.e., sequential arrangement and periodical arrangement (see Fig. 1). Following a recap of the model and formalism that relates the mean return time with the number of energy levels, we derived the general formulas of the eigenvalues and eigenvectors of the ring system via the perturbation theory [46] (see Sec. II). For the two types of spatial distributions of perturbations, the mean and variance of the first return time are investigated (see Figs. 2–4 and Table I). In the case of sequentially arranged perturbations, we found the staircase pattern of the truncated mean return time (see definition below and Fig. 3). Under the symmetry-preserving initial condition, the perturbations do not change the mean and variance of the first return time. In the case of periodically arranged perturbations, we summarized in a table the values of the mean return time, for different parameters that determine the symmetry of the system (see Table I). To further understand the influence of perturbations on the detection time statistics, we also discussed the first detection probability F_n , namely, the distribution of the first detection time, for sequentially or periodically perturbed rings. Besides the monotonic decrease of the decay rate of F_n as the perturbation strength increases (see Fig. 6), we found the coincidence of F_n for a symmetric setup (see Figs. 8 and 9).

The rest of this paper is organized as follows. In Sec. II, we elucidate the model and formalism and derive the general formulas of the eigenvalues and eigenvectors of the perturbed ring system by employing time-independent perturbation theory. The main results as mentioned above are elaborated in detail in Sec. III. We close the paper with a summary and discussion in Sec. IV. Detailed calculations

related to the perturbation theory and Table I are presented in Appendixes A and B.

II. MODEL AND GENERAL FORMALISM

A. Model

The system can be represented in Hilbert space \mathcal{H} , and the quantum particle is initialized at state $|x_{\text{in}}\rangle \in \mathcal{H}$. A time-independent Hamiltonian \hat{H} determines the particle dynamics via the Schrödinger equation. We measure the particle state at a sampling period τ to determine whether the particle is at state $|x_d\rangle \in \mathcal{H}$ or not. The stroboscopic measurement is performed via the projection operator $\hat{D} = |x_d\rangle\langle x_d|$. If the detection fails, the amplitude at the target state $|x_d\rangle$ will vanish, and then the wave function will be renormalized and evolve freely for another duration of τ . We continue this “evolution-projection-evolution...” process unless the walker “hits” the detector. Finally, the particle is detected for the first time at the n th attempt. The indeterministic nature of quantum mechanics renders n random, which is defined as the first detection time.

Following this stroboscopic detection protocol [10,11], the first detection amplitude at the n th attempt is

$$\phi_n = \langle x_d | \hat{U}(\tau) [(1 - \hat{D}) \hat{U}(\tau)]^{n-1} | x_{\text{in}} \rangle, \quad (1)$$

where $\hat{U}(\tau) = e^{-i\hat{H}\tau}$ (\hbar is set as 1 here and in what follows) is the unitary evolution operator of the system. The probability of the first detection at the n th attempt is $F_n = |\phi_n|^2$, and the total probability of detection can be written as $P_{\text{det}} = \sum_{n=1}^{\infty} F_n$. We note that P_{det} can be less than 1, indicating that the walker could evade detection, and the mean detection time can be defined as $\langle n \rangle = \sum_{n=1}^{\infty} n F_n / P_{\text{det}}$. In order to get F_n numerically, we derive from Eq. (1) and get the quantum renewal equation [18,19]

$$\phi_n = \langle x_d | \hat{U}(n\tau) | x_{\text{in}} \rangle - \sum_{m=1}^{n-1} \langle x_d | \hat{U}[(n-m)\tau] | x_d \rangle \phi_m. \quad (2)$$

This equation shows that the first detection amplitude is equal to the measurement-free transition amplitude $\langle x_d | \hat{U}(n\tau) | x_{\text{in}} \rangle$ subtracting the measurement-free return amplitude $\langle x_d | \hat{U}[(n-m)\tau] | x_d \rangle$ propagating from the prior first detection amplitude ϕ_m ($m < n$). This is also the spirit of the classical renewal equation, with a replacement of the probabilities to amplitude [1].

B. Generating function

In practice, it is more convenient to get ϕ_n with its generating function [19,47], i.e., employing the discrete Laplace transform or Z transform

$$\hat{\phi}(z) = \sum_{n=1}^{\infty} z^n \phi_n = \frac{\langle x_d | \hat{U}(z) | x_{\text{in}} \rangle}{1 + \langle x_d | \hat{U}(z) | x_d \rangle}, \quad (3)$$

where $\hat{U}(z) = \sum_{n=1}^{\infty} z^n \hat{U}(n\tau) = \frac{ze^{-i\hat{H}\tau}}{1 - ze^{-i\hat{H}\tau}}$. Upon substituting this form of $\hat{U}(z)$ into Eq. (3) we obtain

$$\hat{\phi}(z) = \frac{\langle x_d | \frac{1}{z^{-1}e^{i\hat{H}\tau} - 1} | x_{\text{in}} \rangle}{1 + \langle x_d | \frac{1}{z^{-1}e^{i\hat{H}\tau} - 1} | x_d \rangle}. \quad (4)$$

We can recover ϕ_n using the inversion formula

$$\phi_n = \frac{1}{n!} \frac{d^n}{dz^n} \hat{\phi}(z) \Big|_{z=0} \quad (5)$$

or Cauchy's integral formula

$$\phi_n = \frac{1}{2\pi i} \oint_{|z|=1} \frac{dz}{z^{n+1}} \hat{\phi}(z). \quad (6)$$

Based on whether $|x_d\rangle$ is the same as $|x_{in}\rangle$, we divide the problem into two types: the return problem and the arrival problem. When $|x_d\rangle = |x_{in}\rangle$, it is called the return problem, which is the focus of this paper, and $\hat{\phi}(z)$ can be expressed specifically as

$$\hat{\phi}(z) = \frac{\langle x_d | \hat{U}(z) | x_d \rangle}{1 + \langle x_d | \hat{U}(z) | x_d \rangle}. \quad (7)$$

When $|x_d\rangle \neq |x_{in}\rangle$, it is called the arrival problem, and $\hat{\phi}(z)$ is consistent with Eq. (3).

The total probability of detection P_{det} and the mean return time $\langle n \rangle$ can be expressed as

$$\begin{aligned} P_{det} &= \sum_{n=1}^{\infty} F_n = \sum_{n=1}^{\infty} |\phi_n|^2 \\ &= \frac{1}{2\pi} \int_0^{2\pi} \sum_{k=1}^{\infty} \phi_k^* e^{-ik\theta} \sum_{l=1}^{\infty} \phi_l e^{il\theta} d\theta \\ &= \frac{1}{2\pi} \int_0^{2\pi} |\hat{\phi}(e^{i\theta})|^2 d\theta \end{aligned} \quad (8)$$

and

$$\begin{aligned} \langle n \rangle &= \sum_{n=1}^{\infty} n F_n = \sum_{n=1}^{\infty} n |\phi_n|^2 \\ &= \frac{1}{2\pi} \int_0^{2\pi} \sum_{k=1}^{\infty} \phi_k^* e^{-ik\theta} \left(\frac{1}{i} \frac{\partial}{\partial \theta} \right) \sum_{l=1}^{\infty} \phi_l e^{il\theta} d\theta \\ &= \frac{1}{2\pi i} \int_0^{2\pi} [\hat{\phi}(e^{i\theta})]^* \partial_{\theta} \hat{\phi}(e^{i\theta}) d\theta, \end{aligned} \quad (9)$$

where we set $e^{i\theta} \rightarrow z$ in the analytic extension of the unit circle.

In the return problem, $\hat{\phi}(e^{i\theta})$ is given by

$$\begin{aligned} \hat{\phi}(e^{i\theta}) &= \frac{\langle x_d | \frac{1}{e^{i(\hat{H}\tau-\theta)} - 1} | x_d \rangle}{1 + \langle x_d | \frac{1}{e^{i(\hat{H}\tau-\theta)} - 1} | x_d \rangle} \\ &= \frac{-\frac{1}{2} - \frac{i}{2} \langle x_d | \cot \frac{(\hat{H}\tau-\theta)}{2} | x_d \rangle}{\frac{1}{2} - \frac{i}{2} \langle x_d | \cot \frac{(\hat{H}\tau-\theta)}{2} | x_d \rangle}. \end{aligned} \quad (10)$$

If we write $\hat{u}(\theta) = \langle x_d | \cot \frac{(\hat{H}\tau-\theta)}{2} | x_d \rangle$, which is a real number, Eq. (10) becomes

$$\hat{\phi}(e^{i\theta}) = \frac{1 + i\hat{u}(\theta)}{-1 + i\hat{u}(\theta)}. \quad (11)$$

Obviously, using Eq. (8), we get the total probability of detection $P_{det} = 1$ because of $|\hat{\phi}(e^{i\theta})| = 1$. If we write $\hat{\phi}(e^{i\theta}) = e^{i\varphi(\theta)}$, where $\varphi(\theta) = 2 \arctan[\hat{u}(\theta)] + \pi$, it follows that

$$\hat{\phi}(e^{i\theta}) = -e^{2i \arctan[\hat{u}(\theta)]}. \quad (12)$$

Upon substituting this expression of $\hat{\phi}(e^{i\theta})$ into Eq. (9), we obtain

$$\langle n \rangle = \frac{1}{2\pi} \int_0^{2\pi} \partial_{\theta} (2 \arctan[\hat{u}(\theta)]) d\theta. \quad (13)$$

Exceptional sampling times

The symmetry of the system, whose Hamiltonian governs the quantum walker's dynamics, can cause the degeneracy of energy levels. In addition, exceptional sampling times τ_c give rise to the pseudodegeneracy, i.e., $e^{-iE_k\tau_c} = e^{-iE_l\tau_c}$, between different energy levels. Hence exceptional sampling time τ_c is defined by

$$|E_k - E_l| \tau_c = 2\pi n, \quad (14)$$

where n is an integer. E_k and E_l are the eigenvalues of the system's Hamiltonian. The pseudodegeneracy leads to non-analytic behaviors at those exceptional sampling times τ_c ; namely, the mean $\langle n \rangle$ in the return case exhibits discontinuous transition, which is accompanied by diverging variance in the vicinity [19,21]. In the arrival problem, $\langle n \rangle$ and the variance of n both diverge [23].

C. Rings with perturbations

We study a nearest-neighbor tight-binding model of finite rings with perturbations in this paper. We first introduce the Hamiltonian of a finite ring with N sites,

$$H_0 = -\gamma \sum_{x=0}^{N-1} (|x\rangle \langle x+1| + |x+1\rangle \langle x|). \quad (15)$$

This equation describes a quantum walker hopping between nearest neighbors on a one-dimensional N -site ring, where γ is the hopping rate between nearest sites. In this paper, we set $\gamma = 1$. This ring system possesses translational invariance, namely, $|0\rangle = |N\rangle$. The eigenvalues of this Hamiltonian H_0 are $E_l^{(0)} = -2 \cos \frac{2\pi l}{N}$, and the corresponding eigenvectors are $|E_l^{(0)}\rangle = \frac{1}{\sqrt{N}} \sum_{x=0}^{N-1} e^{-i\frac{2\pi l}{N}x} |x\rangle$, with $l = 0, 1, \dots, N-1$ [48]. When $l+k=N$ and $l \neq k$, E_l and E_k are a pair of degenerate energy levels. Hence the number of distinct energy levels is $\frac{N+2}{2}$ when N is even and $\frac{N+1}{2}$ when N is odd.

Recently, the model of finite rings has been studied in the return problem [18,19]. For the case of finite rings, the quantum walk as shown above [see Eqs. (8) and (12)] is always recurrent in the return problems, i.e., $P_{det} = 1$. Aside from isolated exceptional sampling times τ_c , the mean return time is independent of the general sampling time τ , and it just depends on the number of sites,

$$\langle n \rangle = \begin{cases} \frac{N+2}{2}, & N \text{ is even} \\ \frac{N+1}{2}, & N \text{ is odd.} \end{cases} \quad (16)$$

Here, we can see that $\langle n \rangle$ is the number of distinct energy levels of the system. However, Eq. (16) is not applicable for exceptional sampling times. According to Eq. (14), whenever two modes $\exp(iE_k\tau)$ are identical when strobed at each period τ_c , the value of $\langle n \rangle$ is reduced by unity. Therefore the mean return time is less than or equal to the number of energy levels.

Apparently, the results of the perturbed system are different from the above results [21]. We next consider a finite ring system with perturbations. Assume that perturbations are located at sites ξ_j with $j = 1, 2, \dots, m$ and $\xi_j \in M$. M is the set of sites at which the perturbations are located. The energy of perturbations is a small constant $-\gamma\epsilon$, and $\epsilon^2 \ll 1$. Then, the total Hamiltonian of the system with perturbations is

$$H = H_0 + H', \quad (17)$$

where H' is the Hamiltonian of perturbations and $H' = -\gamma\epsilon \sum_{j=1}^m |\xi_j\rangle\langle\xi_j|$.

Eigenvalues and eigenvectors of the perturbed rings

The eigenvalues of the total Hamiltonian in Eq. (17) and their corresponding eigenvectors can be obtained approximately with perturbation theory. We study a finite ring model with even sites, i.e., N is even, and the different eigenvalues can be calculated by $E_l^{(0)} = -2 \cos \frac{2\pi l}{N}$ with $l = 0, 1, \dots, \frac{N}{2}$ [48]. Apparently, this system has two nondegenerate energy levels, $E_0^{(0)}$ and $E_{\frac{N}{2}}^{(0)}$, and their corresponding eigenvectors are

$$|E_0^{(0)}\rangle = \frac{1}{\sqrt{N}} \sum_{x=0}^{N-1} |x\rangle, \quad (18)$$

$$|E_{\frac{N}{2}}^{(0)}\rangle = \frac{1}{\sqrt{N}} \sum_{x=0}^{N-1} (-1)^x |x\rangle. \quad (19)$$

The rest of the energy levels ($l \neq 0, \frac{N}{2}$) are doubly degenerate, and each energy level corresponds to two degenerate eigenvectors

$$|E_{l1}^{(0)}\rangle = \frac{1}{\sqrt{N}} \sum_{x=0}^{N-1} e^{i\frac{2\pi l}{N}x} |x\rangle, \quad (20)$$

$$|E_{l2}^{(0)}\rangle = \frac{1}{\sqrt{N}} \sum_{x=0}^{N-1} e^{i\frac{2\pi(N-l)}{N}x} |x\rangle. \quad (21)$$

In this paper, the approximate results of eigenvalues and the corresponding eigenvectors are accurate to the second-order correction for the nondegenerate cases. For the degenerate cases, the approximate results of eigenvalues and the corresponding eigenvectors are accurate to the first-order correction. For the nondegenerate energy levels E_0 and $E_{\frac{N}{2}}$, their first-order correction can be expressed as

$$E_l^{(1)} = -\epsilon \sum_{j=1}^m |\langle \xi_j | E_l^{(0)} \rangle|^2 = -\epsilon \frac{m}{N}, \quad (22)$$

where $l = 0$ or $\frac{N}{2}$. The first-order correction of the corresponding eigenvector is

$$|E_l^{(1)}\rangle = \sum_{n \neq l} \sum_{\mu=1}^{g_n} \frac{H'_{n\mu,l}}{E_l^{(0)} - E_n^{(0)}} |E_{n\mu}^{(0)}\rangle, \quad (23)$$

where $H'_{n\mu,l} = \langle E_{n\mu}^{(0)} | H' | E_l^{(0)} \rangle$ and g_n is the degeneracy of E_n .

Furthermore, we explore the second-order correction of eigenvalues and eigenvectors for the nondegenerate energy levels $E_0^{(0)}$ and $E_{\frac{N}{2}}^{(0)}$. The correction of the eigenvalue is given

by

$$E_l^{(2)} = \sum_{n \neq l} \sum_{\mu=1}^{g_n} \frac{|H'_{n\mu,l}|^2}{E_l^{(0)} - E_n^{(0)}}. \quad (24)$$

The second-order correction of the eigenvector is given by

$$|E_l^{(2)}\rangle = \sum_{n \neq l} \sum_{\mu=1}^{g_n} \left[\sum_{m \neq l} \sum_{i=1}^{g_m} \frac{H'_{n\mu,mi} H'_{mi,l}}{(E_l^{(0)} - E_n^{(0)})(E_l^{(0)} - E_m^{(0)})} - \frac{H'_{mi,l} H'_{l,i}}{(E_l^{(0)} - E_n^{(0)})^2} \right] |E_{n\mu}^{(0)}\rangle. \quad (25)$$

Then, using Eqs. (18)–(25), we can obtain the second-order corrected eigenvalues and eigenvectors. See Appendix A for the specific expressions of eigenvalues and eigenvectors of the ring Hamiltonian.

As to the degenerate energy levels, the degeneracy is removed due to the presence of perturbations. We can obtain the first-order correction of eigenvalue $E_{l\alpha}^{(1)}$ with secular equation

$$\begin{vmatrix} H'_{l1,l1} - E_{l\alpha}^{(1)} & H'_{l1,l2} \\ H'_{l2,l1} & H'_{l2,l2} - E_{l\alpha}^{(1)} \end{vmatrix} = 0, \quad (26)$$

where $H'_{l1,l1} = H'_{l2,l2} = -\epsilon \frac{m}{N}$ and $H'_{l1,l2} = H'_{l2,l1} = -\frac{\epsilon}{N} \sum_{j=1}^m e^{-i4\pi \xi_j l / N}$. Equation (26) can be solved exactly to obtain

$$E_{l\alpha}^{(1)} = -\frac{\epsilon}{N} \left(m + (-1)^\alpha \left| \sum_{j=1}^m e^{i\frac{4\pi \xi_j l}{N}} \right| \right). \quad (27)$$

Because the degeneracy of $E_{l\alpha}$ is 2 in our model, α in Eq. (27) is equal to 1 or 2.

According to the perturbation theory, the new zero-order eigenvector of degenerate energy levels can be expressed as

$$|E_{l\alpha}^{(0)}\rangle = \sum_{i=1}^{g_l} a_{\alpha i} |E_{li}^{(0)}\rangle, \quad (28)$$

where g_l is the degeneracy of E_l and $i = 1, 2$. The coefficient $a_{\alpha i}$ can be determined by solving the equation

$$\sum_{i,i'=1}^{g_l} (H'_{li',li} - E_{l\alpha}^{(1)} \delta_{li',li}) a_{\alpha i} = 0. \quad (29)$$

Upon substituting for $E_{l\alpha}^{(1)}$ from Eq. (28) and $H'_{li',li}$ into Eq. (29), we obtain $(a_{11} \ a_{12})^T = \frac{\sqrt{2}}{2} (-e^{i\beta} \ 1)^T$ and $(a_{21} \ a_{22})^T = \frac{\sqrt{2}}{2} (e^{i\beta} \ 1)^T$, where T means matrix transposition and $e^{i\beta} = \frac{\sum_{j=1}^m e^{-i4\pi \xi_j l / N}}{|\sum_{j=1}^m e^{-i4\pi \xi_j l / N}|}$.

The first-order correction of the corresponding eigenvector is given by

$$|E_{l\alpha}^{(1)}\rangle = \sum_{n \neq l} \sum_{i=1}^{g_l} \sum_{\mu=1}^{g_n} a_{\alpha i} \frac{H'_{n\mu,li}}{E_l^{(0)} - E_n^{(0)}} |E_{n\mu}^{(0)}\rangle. \quad (30)$$

Hence, in the sense of the first-order correction, if the degeneracy of E_l is removed, so that the twofold energy level E_l splits into two energy levels, we can obtain the first-order corrected eigenvalues and eigenvectors with Eqs. (27)–(30) (see details in Appendix A).

However, when the degeneracy is maintained, namely, $E_{l1}^{(1)} = E_{l2}^{(1)}$, we cannot obtain $a_{\alpha i}$ via Eq. (29) anymore, and we cannot get the new zero-order eigenvector with Eq. (28). In the remainder of this section, we adopt another method [46] to determine the coefficient $a_{\alpha i}$ when the degeneracy is removed in the second-order correction.

We first calculate the second-order correction of eigenvalue $E_{l\alpha}^{(2)}$. In order to get $E_{l\alpha}^{(2)}$, we need to solve the following equation:

$$\det \left| \sum_{n \neq l} \sum_{\mu=1}^{g_n} \frac{\hat{H}'_{n\mu,li} \hat{H}'_{li',n\mu}}{E_l^{(0)} - E_n^{(0)}} - E_{l\alpha}^{(2)} \delta_{li',li} \right| = 0. \quad (31)$$

We obtain

$$E_{l\alpha}^{(2)} = \sum_{n \neq l} \sum_{\mu=1}^{g_n} \frac{\hat{H}'_{n\mu,l1} \hat{H}'_{l1,n\mu}}{E_l^{(0)} - E_n^{(0)}} + (-1)^\alpha \left| \sum_{n \neq l} \frac{\hat{H}'_{n\mu,l1} \hat{H}'_{l2,n\mu}}{E_l^{(0)} - E_n^{(0)}} \right|. \quad (32)$$

Because of $\hat{H}'_{n\mu,l1}$, $\hat{H}'_{l1,n\mu}$, $\hat{H}'_{n\mu,l1}$, and $\hat{H}'_{l2,n\mu} \sim \epsilon$, $E_{l\alpha}^{(2)}$ is a small quantity and approximately equals zero. Upon substituting Eq. (32) into the equation

$$\sum_{i,i'=1}^{g_l} \left(\sum_{n \neq l} \sum_{\mu=1}^{g_n} \frac{\hat{H}'_{n\mu,li} \hat{H}'_{li',n\mu}}{E_l^{(0)} - E_n^{(0)}} - E_{l\alpha}^{(2)} \delta_{li',li} \right) a_{\alpha i} = 0, \quad (33)$$

we obtain $(a_{11} \ a_{12})^T = \frac{\sqrt{2}}{2} (-e^{i\gamma} \ 1)^T$ and $(a_{21} \ a_{22})^T = \frac{\sqrt{2}}{2} (e^{i\gamma} \ 1)^T$, where $e^{i\gamma} = \frac{\sum_{n \neq l} \sum_{\mu=1}^{g_n} \frac{\hat{H}'_{n\mu,l1} \hat{H}'_{l2,n\mu}}{E_l^{(0)} - E_n^{(0)}}}{|\sum_{n \neq l} \sum_{\mu=1}^{g_n} \frac{\hat{H}'_{n\mu,l1} \hat{H}'_{l2,n\mu}}{E_l^{(0)} - E_n^{(0)}}|}$. Using

Eqs. (28) and (30), we obtain the new zero-order eigenvectors $|E_{l\alpha}^{(0)}\rangle$ and the first-order correction eigenvector $|E_{l\alpha}^{(1)}\rangle$.

We consider the approximate results of eigenvalues and the corresponding eigenvectors being accurate to the first-order correction for the degenerate cases. When the degeneracy is removed in the second order but not in the first order, namely, $E_{l1} = E_{l2} = -(2 \cos \frac{2\pi l}{N} + \epsilon \frac{m}{N})$, we can obtain the first-order corrected eigenvectors using the results of $|E_{l\alpha}^{(0)}\rangle$ and $|E_{l\alpha}^{(1)}\rangle$ with Eqs. (28) and (30)–(33) (see details in Appendix A).

Similarly, if the degeneracy is removed at higher order, this method can also be extended to higher-order perturbation cases in solving the eigenvectors.

III. RESULTS

A. The mean return time

The mean return time $\langle n \rangle$ may increase as the number of energy levels increases due to the removal of the degeneracy. When the degeneracy is not removed, namely, the number of energy levels is minimal, the mean return time $\langle n \rangle$ must be minimal. Whether or not the degenerate energy levels split will depend on the summation in Eq. (27) being zero. If the summation is zero, the degenerate energy levels do not split. Since the perturbation potential energies have the same amplitude in this paper, the summation only depends on the sites at which the perturbations are located. In the following sections, we will study two special arrangements of perturbations on a ring system: the sequential arrangement of perturbations and the periodic arrangement of perturbations [44].

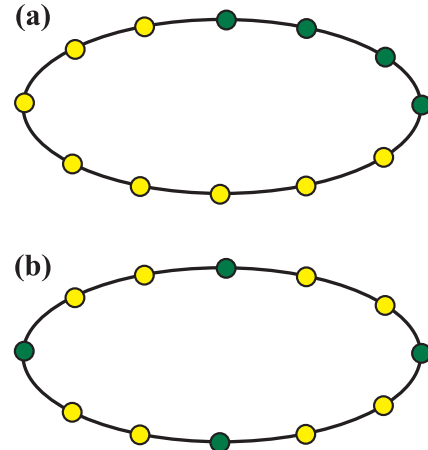


FIG. 1. Examples of sequential (a) and periodic (b) arrangements of $m = 4$ perturbations on a ring of size $N = 12$. The green circles represent the perturbed sites.

1. Sequentially perturbed rings

First, we consider the case of sequential arrangement of perturbations, as illustrated in Fig. 1(a). We assume that the ring has N sites and m perturbations, and the j th perturbation is located at the $\xi_j = j$ th site, where $j = 0, 1, \dots, m - 1$. Upon substituting for $\xi_j = j$ in Eq. (27), we obtain

$$E_{l\alpha}^{(1)} = -\frac{\epsilon}{N} \left(m + (-1)^\alpha \left| \sum_{\xi_j=0}^{m-1} e^{i \frac{4\pi \xi_j l}{N}} \right| \right). \quad (34)$$

The summation part in Eq. (34) can be reduced to

$$\sum_{\xi_j=0}^{m-1} e^{i \frac{4\pi \xi_j l}{N}} = \frac{1 - e^{i \frac{4\pi m l}{N}}}{1 - e^{i \frac{4\pi l}{N}}} = \frac{\sin \frac{2\pi l m}{N}}{\sin \frac{2\pi l}{N}} \times e^{i \frac{2\pi l(m-1)}{N}}, \quad (35)$$

where $l \in [1, \frac{N}{2} - 1]$. When the size of the ring is twice the number of perturbations, i.e., $N = 2m$, we have $\sum_{\xi_j=0}^{m-1} e^{i \frac{4\pi l}{N} \xi_j} = 0$, and then $E_{l1}^{(1)} = E_{l2}^{(1)} = -\epsilon \frac{m}{N}$. This means that the degenerate energy levels do not split, and the number of energy levels in this perturbed system is equal to that in the unperturbed system. The only difference is that the energy for each level shifts by the same value $-\epsilon \frac{m}{N}$. Hence the mean return time does not change, and the exceptional sampling times in the perturbed system are also the same as in the unperturbed system. In Fig. 2, we compare the mean return time $\langle n \rangle$ and the variance of n in the unperturbed ring system and sequentially perturbed ring system with the sizes $N = 6$ and 8. The results show that even if the size of the ring is different, $\langle n \rangle$ and the variance of n are consistent in the perturbed and unperturbed systems.

However, Eq. (34) is the approximate result, and Fig. 2 shows the results of the finite summation with the attempt number $\mathcal{N} = 30\,000$. As to the case of exact solutions, every pair of degenerate energy levels can split into two energy levels with a very small difference. As shown in Fig. 3, for the sequentially perturbed ring system with the sizes $N = 6$ and 8, it can be found that, with the increase in the attempt number \mathcal{N} , $\langle n \rangle_{\mathcal{N}} = \sum_{n=1}^{\mathcal{N}} n F_n$ has two plateaus at $\frac{N}{2} + 1$ and N in most cases. For the small number of attempts, the degenerate

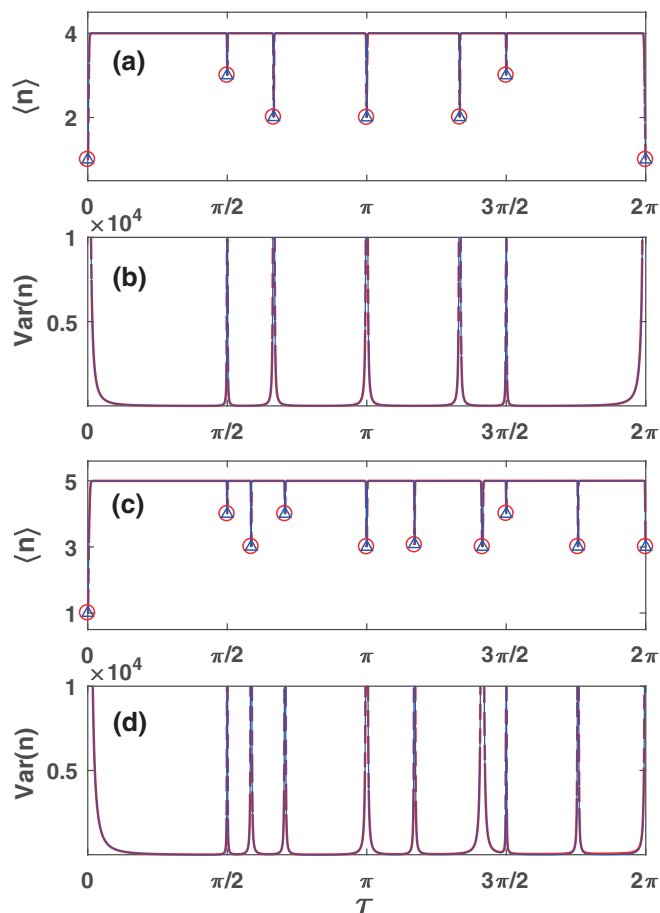


FIG. 2. In the quantum return problem, the mean return time $\langle n \rangle$ and the variance of n vs τ for the cases of a sequentially perturbed system and an unperturbed system. The size of the ring systems is set at $N = 6$ in (a) and (b) and $N = 8$ in (c) and (d). The initial positions are set at $x_{\text{in}} = 1$ in (a) and (b) and $x_{\text{in}} = 2$ in (c) and (d). The red dashed curves show the results for $m = \frac{N}{2}$ sequentially arranged perturbations with amplitude $\epsilon = 0.025$. The blue curves are the results for the case of the unperturbed system. In (a) and (c), the open circles and triangles are the singularities for the perturbed and unperturbed systems, respectively.

energy levels cannot be resolved and appear as one, resulting in a coarse-grained quantization. However, when $N = 6$ and $x_{\text{in}} = 1$ or 4 , the mean return time always equals $\frac{N}{2} + 1$. This is because the choice of the initial condition does not break the reflection symmetry of the system.

2. Periodically perturbed rings

Next, we consider the case of a periodic arrangement of perturbations, as illustrated in Fig. 1(b). We assume that the j th perturbation is located at the $\xi_j = (a * j)$ th site, where a is the interval between adjacent perturbations and $j = 0, 1, \dots, m - 1$. The relation between N, m , and a is $N = ma$. Upon substituting for $\xi_j = a * j$ in Eq. (27), we obtain

$$E_{l\alpha}^{(1)} = -\frac{\epsilon}{N} \left(m + (-1)^\alpha \left| \sum_{j=0}^{m-1} e^{i\frac{4\pi l}{N} a j} \right| \right). \quad (36)$$

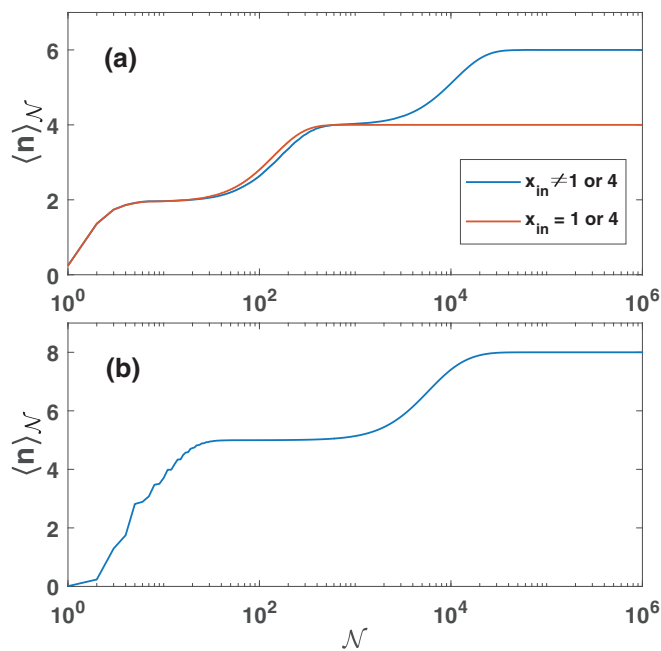


FIG. 3. For $m = \frac{N}{2}$ sequentially arranged perturbations with amplitude $\epsilon = 0.025$, the mean return time $\langle n \rangle$ vs the attempt number n when $\tau = 90$. The size of the ring systems is set at $N = 6$ in (a) and $N = 8$ in (b). In (a), the blue curve and the orange curve show the results for the initial conditions $x_{\text{in}} \neq 1$ or 4 and $x_{\text{in}} = 1$ or 4 , respectively. The blue curve has two plateaus at $\langle n \rangle = 4$ and 6 , and the orange curve only has a plateau at $\langle n \rangle = 4$. In (b), the blue curve shows the results for arbitrary initial conditions, and it has two plateaus at $\langle n \rangle = 5$ and 8 .

For the general case, i.e., $e^{i\frac{4\pi l}{N} a} \neq 1$, the summation part in Eq. (36) takes the simple form

$$\sum_{j=0}^{m-1} e^{i\frac{4\pi al}{N} j} = \frac{1 - e^{i\frac{4\pi mal}{N}}}{1 - e^{i\frac{4\pi al}{N}}} = \frac{\sin \frac{2\pi al m}{N}}{\sin \frac{2\pi al}{N}} \times e^{i\frac{2\pi al(m-1)}{N}} = 0. \quad (37)$$

In this case, the energy for each level also shifts by the same value $-\epsilon \frac{m}{N}$ as in the last case. There is no degenerate energy level split. The difference between each pair of energy levels does not change; that is, the mean return time $\langle n \rangle$ and exceptional sampling times are unchanged. As shown in Figs. 4(a) and 4(b), we compare the mean return time $\langle n \rangle$ and the variance of n in the unperturbed system and periodically perturbed system with $N = 6$ and $a = 2$. In the two systems, $\langle n \rangle$ and the variance of n are still consistent.

However, when $\frac{2la}{N}$ is an integer, we have $e^{i\frac{4\pi l}{N} a} = 1$, and

$$\sum_{j=0}^{m-1} e^{i\frac{4\pi l}{N} a j} = m. \quad (38)$$

Upon substituting Eq. (38) into Eq. (36), we get the first-order correction $E_{l\alpha}^{(1)} = 0$ or $-\epsilon \frac{2m}{N}$. This means that the corresponding degenerate energy level splits. Due to the energy level splitting, the numbers of energy levels and exceptional sampling times of the perturbed system are different from those of the unperturbed system. As shown in Figs. 4(c) and 4(d), we compare the mean return time $\langle n \rangle$ and the variance of n in an unperturbed system and a periodically perturbed system with

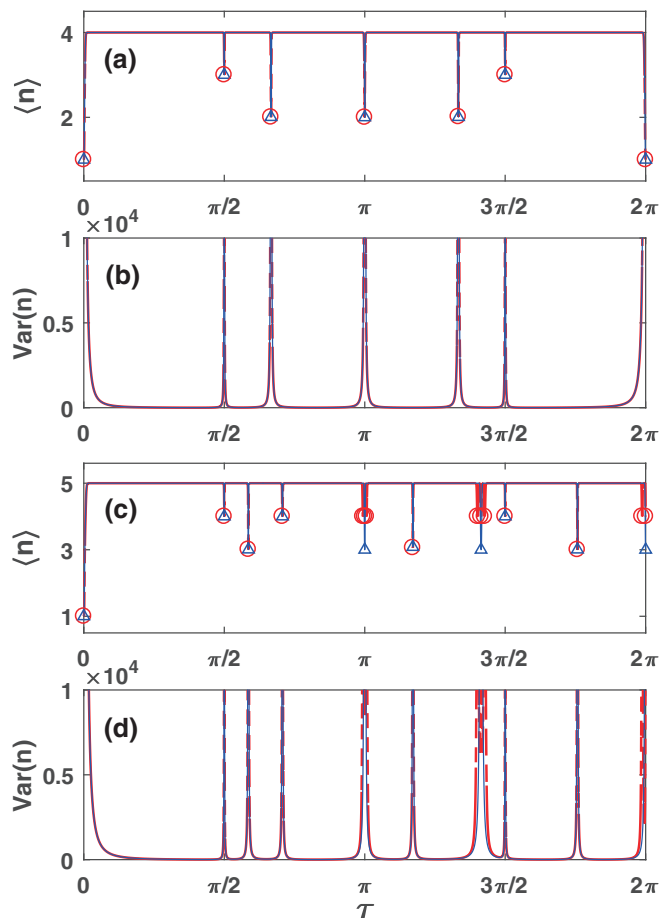


FIG. 4. In the quantum return problem, the mean return time $\langle n \rangle$ and the variance of n vs τ for the cases of a periodically perturbed system and an unperturbed system. In (a) and (b), $N = 6$; in (c) and (d), $N = 8$. The initial positions are set at $x_{\text{in}} = 0$ in (a)–(d). The red dashed curves show the results for $m = \frac{N}{2}$ periodically arranged perturbations with amplitude $\epsilon = 0.025$. The blue curves are the results for the case of an unperturbed system. In (a) and (c), the open circles and triangles are the singularities for the perturbed and unperturbed systems, respectively.

$N = 8$ and $a = 2$. The results show that the mean return time $\langle n \rangle$ is the same, except for exceptional sampling time, and the variances of n are not coincident in the two systems as a pair of degenerate energy levels split up.

From Eq. (36), we find that the ring size N and the interval a can affect degenerate energy levels splitting up, and they may change the mean return time $\langle n \rangle$. In addition, when some pairs of degenerate energy levels split up, the mean return time $\langle n \rangle$ for different initial positions x_{in} may show different results [21]. We now show how the size of the ring N , the interval a , and the initial position x_{in} influence the mean return time $\langle n \rangle$. The detailed results are shown in Table I (the detailed derivation is given in Appendix B). The upper half and the lower half of the table show the results for $\frac{N}{2}$ being even and odd, respectively. In the table, Δx is the minimum distance between the initial position x_{in} and the position of perturbation ξ_j , i.e., $\Delta x = |x_{\text{in}} - \xi_j|_{\text{min}}$. Apparently, $0 \leq \Delta x \leq \frac{a}{2}$. We can find that N_E , the number of energy levels, has two possible values, $\frac{N}{2} + 1$ and $\frac{N}{2} + 1 + s$, where s is the number of split

TABLE I. The mean return time $\langle n \rangle$ and the number of energy levels N_E for a quantum walker on a periodically perturbed ring. $\Delta x = |x_{\text{in}} - \xi_j|_{\text{min}}$. s is the number of split degenerate energy levels. b_i is a divisor of a .

a	Δx	N_E	$\langle n \rangle$
$\frac{N}{2}$ is even			
Even			
2	any	$\frac{N}{2} + 1 + s$	$\frac{N}{2} + 1$
4	0 or $\frac{a}{2}$	$\frac{N}{2} + 1 + s$	$\frac{N}{2} + 1$
	other	$\frac{N}{2} + 1 + s$	$\frac{N}{2} + 1 + s$
≥ 6	0 or $\frac{a}{2}$	$\frac{N}{2} + 1 + s$	$\frac{N}{2} + 1$
	nb_i	$\frac{N}{2} + 1 + s$	$\frac{N}{2} + 1 + s - (b_i - 1)$
	other	$\frac{N}{2} + 1 + s$	$\frac{N}{2} + 1 + s$
Odd			
Prime number	0	$\frac{N}{2} + 1 + s$	$\frac{N}{2} + 1$
	other	$\frac{N}{2} + 1 + s$	$\frac{N}{2} + 1 + s$
Composite number	0	$\frac{N}{2} + 1 + s$	$\frac{N}{2} + 1$
	nb_i	$\frac{N}{2} + 1 + s$	$\frac{N}{2} + 1 + s - (b_i - 1)$
	other	$\frac{N}{2} + 1 + s$	$\frac{N}{2} + 1 + s$
$\frac{N}{2}$ is odd			
Even			
2	any	$\frac{N}{2} + 1$	$\frac{N}{2} + 1$
≥ 6	0 or $\frac{a}{2}$	$\frac{N}{2} + 1 + s$	$\frac{N}{2} + 1$
	nb_i	$\frac{N}{2} + 1 + s$	$\frac{N}{2} + 1 + s - (b_i - 1)$
	other	$\frac{N}{2} + 1 + s$	$\frac{N}{2} + 1 + s$
Odd			
Prime number	0	$\frac{N}{2} + 1 + s$	$\frac{N}{2} + 1$
	other	$\frac{N}{2} + 1 + s$	$\frac{N}{2} + 1 + s$
Composite number	0	$\frac{N}{2} + 1 + s$	$\frac{N}{2} + 1$
	nb_i	$\frac{N}{2} + 1 + s$	$\frac{N}{2} + 1 + s - (b_i - 1)$
	other	$\frac{N}{2} + 1 + s$	$\frac{N}{2} + 1 + s$

degenerate energy levels. Here, $s = a - 1$ when m is even, and $s = \frac{a}{2} - 1$ when m is odd. The mean return time $\langle n \rangle$ is less than or equal to N_E , and $\langle n \rangle$ has three possible results. They are $\frac{N}{2} + 1$, $\frac{N}{2} + 1 + s$, and $\frac{N}{2} + 1 + s - (b_i - 1)$, where the integer b_i is a divisor of a , and $1 < b_i < \frac{a}{2}$.

However, for the case of $a = 2$, there is only one result when $\frac{N}{2}$ is odd or even. When $a = 2$, the degenerate energy level splits under the condition of $\frac{N}{2}$ being even, and this means N_E increasing accordingly. However, when $a = 2$ and $\frac{N}{2}$ is odd, there is no degenerate energy level splitting. No matter whether the energy level splits or not, the mean return time $\langle n \rangle$ remains unchanged, and it is equal to the mean return time in the unperturbed ring, i.e., $\langle n \rangle = \frac{N}{2} + 1$. In addition, compared with the case of a being a prime number, $\langle n \rangle$ has an extra possible value of $\frac{N}{2} + 1 + s - (b_i - 1)$ when a is a composite number.

In fact, when the periodic arrangement of perturbations does not break the symmetry of the system, the mean return time $\langle n \rangle$ is consistent in the perturbed and unperturbed systems. As discussed above, the initial position x_{in} is a key variable which influences the symmetry of the system. In the ring system with periodically arranged perturbations, when $\frac{N}{2}$

is even and $x_{\text{in}} = \frac{ka}{2}$, or when $\frac{N}{2}$ is odd and $x_{\text{in}} = ka$, where k is an integer, the symmetry of the perturbed system is preserved.

When the perturbation amplitude ϵ is much less than 1, the terms including the first-order small quantity of ϵ in the eigenvectors calculated with perturbation theory can be ignored. Hence the first-order correction is considered in the calculation of the eigenvalues, and the zero-order correction is considered in the calculation of corresponding eigenvectors. When a and $\frac{N}{2}$ are even, the conclusions in Table I are not always applicable. The decrease in the perturbation strength ϵ may change the mean return time $\langle n \rangle$ at some special initial position, and the maximum of $\langle n \rangle$ is no longer $\frac{N}{2} + 1 + s$ but $\frac{N}{2} + s$.

3. The winding number of $\hat{\phi}(e^{i\theta})$ in perturbed systems

In Table I, we can find that the number of energy levels is not necessarily equal to the mean return time. We will discuss $\langle n \rangle$ in this section. After simplifying Eq. (10), we have

$$\hat{\phi}(e^{i\theta}) = \frac{e^{i\theta} \sum_{k=1}^w p_k / (e^{iE_k\tau} - e^{i\theta})}{\sum_{k=1}^w p_k e^{iE_k\tau} / (e^{iE_k\tau} - e^{i\theta})}, \quad (39)$$

where the overlaps $p_k = \sum_{l=1}^{g_k} |\langle x_d | E_{kl} \rangle|^2$, g_k is the degeneracy of the eigenvalue E_k , and w is the amount of nonzero p_k corresponding to different energy phases $e^{iE_k\tau}$. For general sampling time, if all p_k are nonzero, w is exactly equal to the dimension of the Hilbert space; however, if there is a p_k that is zero, w will be reduced by 1. In addition, when we set τ to be an exceptional sampling time, namely, there exists a pair of energy levels E_k, E_l satisfying $|E_k - E_l|\tau = 2\pi n$, i.e., $e^{iE_k\tau} = e^{iE_l\tau}$, w will be reduced by 1.

We may replace $e^{i\theta}$ by z , and Eq. (39) can be rewritten as $\hat{\phi}(z) = \frac{\mathcal{N}(z)}{\mathcal{D}(z)}$, where $\mathcal{N}(z)$ and $\mathcal{D}(z)$ are given by

$$\mathcal{N}(z) = z \sum_{k=1}^w p_k \prod_{\substack{j=1 \\ j \neq k}}^w (e^{iE_j\tau} - z), \quad (40)$$

$$\mathcal{D}(z) = \sum_{k=1}^w p_k e^{iE_k\tau} \prod_{\substack{j=1 \\ j \neq k}}^w (e^{iE_j\tau} - z), \quad (41)$$

respectively. The relation between $\mathcal{N}(z)$ and $\mathcal{D}(z)$ is

$$\mathcal{D}(z) = e^{i \sum_{k=1}^w E_k\tau} \cdot (-1)^{w-1} z^w \left[\mathcal{N}\left(\frac{1}{z^*}\right) \right]^*. \quad (42)$$

Here, we can rewrite $\mathcal{N}(z)$ in another form,

$$\mathcal{N}(z) = z \prod_{i=1}^{w-1} (z_i - z), \quad (43)$$

where $\{z_i\}$ are the zeros of $\hat{\phi}(z)$ and lie inside the unit circle on the complex plane. Upon combining Eqs. (42) and (43), after some rearrangement, we obtain

$$\hat{\phi}(z) = e^{-i \sum_{k=1}^w E_k\tau} \cdot \frac{z \prod_{i=1}^{w-1} (z_i - z)}{\prod_{i=1}^{w-1} (1 - z_i^* z)}. \quad (44)$$

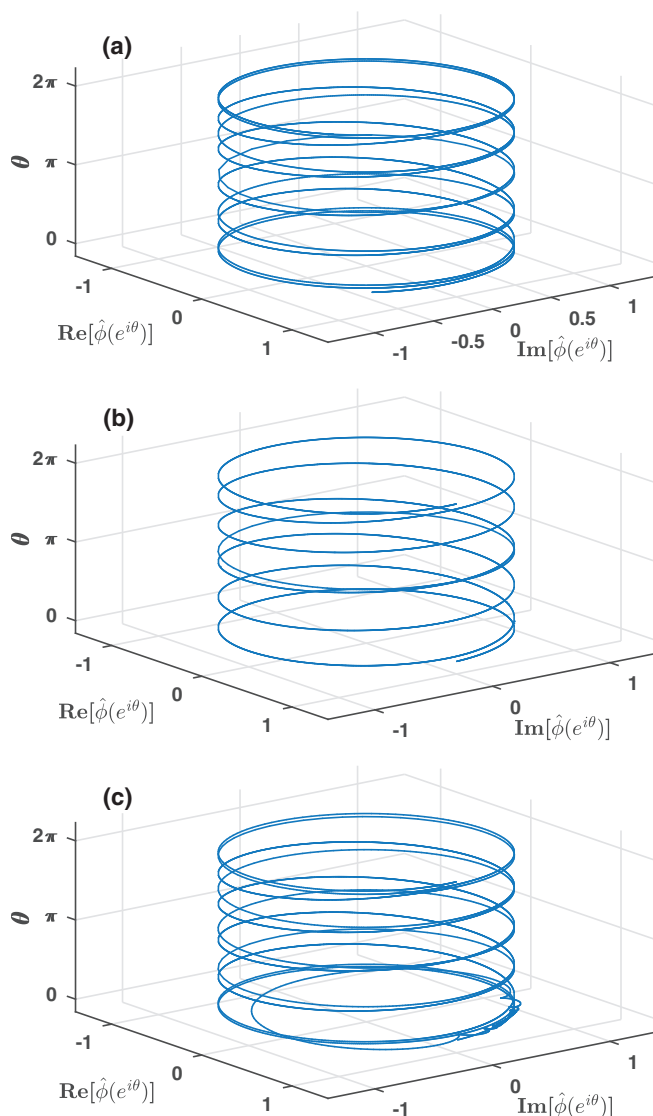


FIG. 5. Three-dimensional plot of $\hat{\phi}(e^{i\theta})$ in the periodic arrangement of two perturbations on the ring of size $N = 12$. The initial positions x_{in} are set at $x_{\text{in}} = 2, 3$, and 5 in (a)–(c), respectively. The curves show that the winding numbers are 11, 7, and 12 in (a)–(c), respectively.

Then, with $|\hat{\phi}(e^{i\theta})| = 1$ and using Eq. (9), the mean return time $\langle n \rangle$ can be described by the variable z ,

$$\begin{aligned} \langle n \rangle &= \frac{1}{2\pi} \int_{-\pi}^{\pi} (-i\partial_{\theta}) \ln[\hat{\phi}(e^{i\theta})] d\theta \\ &= \frac{1}{2\pi i} \oint_{|z|=1} \left[\frac{1}{z} + \sum_{i=1}^{w-1} \left(\frac{1}{z - z_i} + \frac{z_i^* z}{1 - z_i^* z} \right) \right] dz. \end{aligned} \quad (45)$$

According to the residue theorem and after a lengthy derivation, we obtain

$$\langle n \rangle = w. \quad (46)$$

This means that the mean return time is equal to the winding number of $\hat{\phi}(e^{i\theta})$, and this result will be demonstrated in Fig. 5.

Figure 5 shows the curves of $\hat{\phi}(e^{i\theta})$ as a function of the phase θ when the site number $N = 12$ and the distribution period of perturbations $a = 6$ (i.e., perturbed sites are $\xi_1 = 0$ and $\xi_2 = 6$). When the initial positions x_{in} are 2, 3, and 5, the corresponding curves are shown in Figs. 5(a)–5(c), respectively. According to Table I, when x_{in} is 2, 3, and 5, the corresponding mean return time $\langle n \rangle$ is 11, 7, and 12. It can be found that the winding number w is 11, 7, and 12 in Figs. 5(a)–5(c), respectively. These results confirm the conclusion of Eq. (46).

B. The first detection probability

In addition to the mean return time, the probability of the first detection at the n th attempt F_n is also a significant parameter in the return problem. In this section, we will study F_n in perturbed systems.

1. The first detection amplitude

The first detection probability is the modular square of the first detection amplitude, i.e., $F_n = |\phi_n|^2$. Hence we first study the first detection amplitude in perturbed systems. Upon substituting $p_k = \sum_{l=1}^{g_k} | \langle x_d | E_{kl} \rangle |^2$ into Eq. (2), we obtain

$$\phi_n = \sum_{k=1}^w p_k e^{-inE_k\tau} - \sum_{m=1}^{n-1} \sum_{k=1}^w p_k e^{-i(n-m)E_k\tau} \phi_m. \quad (47)$$

We now consider a perturbed ring system with N sites, and the system has $m = \frac{N}{2}$ (being odd) perturbations arranged sequentially. In order to facilitate the analysis, we set the located sites of perturbations $\xi_j \in \{ \text{mod}(\frac{3N-2}{4} + 1, N), \text{mod}(\frac{3N-2}{4} + 2, N), \dots, \text{mod}(\frac{3N-2}{4} + \frac{N}{2}, N) \}$. Hence the central perturbation is at site 0; namely, the perturbed ring system still maintains its symmetry. The inner product of initial state $|0\rangle$ and each eigenvector of the perturbed ring system is given by

$$\langle 0 | E_0 \rangle = \frac{1}{\sqrt{N}} + \frac{\epsilon}{2N\sqrt{N}} \sum_{n \neq 0} g_n \frac{\csc \frac{n\pi}{N} \sin \frac{n\pi}{2}}{1 - \cos \frac{2\pi n}{N}}, \quad (48)$$

$$\langle 0 | E_{\frac{N}{2}} \rangle = \frac{1}{\sqrt{N}} + \frac{\epsilon}{2N\sqrt{N}} \sum_{n \neq \frac{N}{2}} g_n \frac{\sec \frac{n\pi}{N} \sin \frac{(N+2n)\pi}{4}}{1 - \cos \frac{2\pi n}{N}}, \quad (49)$$

$$\langle 0 | E_{l1} \rangle = 0, \quad (50)$$

$$\langle 0 | E_{l2} \rangle = \sqrt{\frac{2}{N}} + \frac{\epsilon}{(2N)^{\frac{3}{2}}} \sum_{n \neq l} g_n \times \frac{\csc \frac{(l-n)\pi}{N} \sin \frac{(l-n)\pi}{2} + \csc \frac{(l+n)\pi}{N} \sin \frac{(l+n)\pi}{2}}{\cos \frac{2\pi l}{N} - \cos \frac{2\pi n}{N}}. \quad (51)$$

These results are acquired with perturbation theory; hence they are approximate results. Coincidentally, Eq. (50) is also the exact solution; this is because the reflection symmetry of the perturbed system is not broken in the initial conditions. Solving for the eigenvalues and the corresponding eigenvectors of the sequentially perturbed system with $N = 6$ and $\epsilon = 0.025$, we find that two eigenvectors of H are $|E_{k1}\rangle = \{0, -0.503115, 0.496865, 0, -0.496865, 0.503115\}$ and $|E_{l1}\rangle = \{0, -0.496865, -0.503115, 0, 0.503115, 0.496865\}$ and

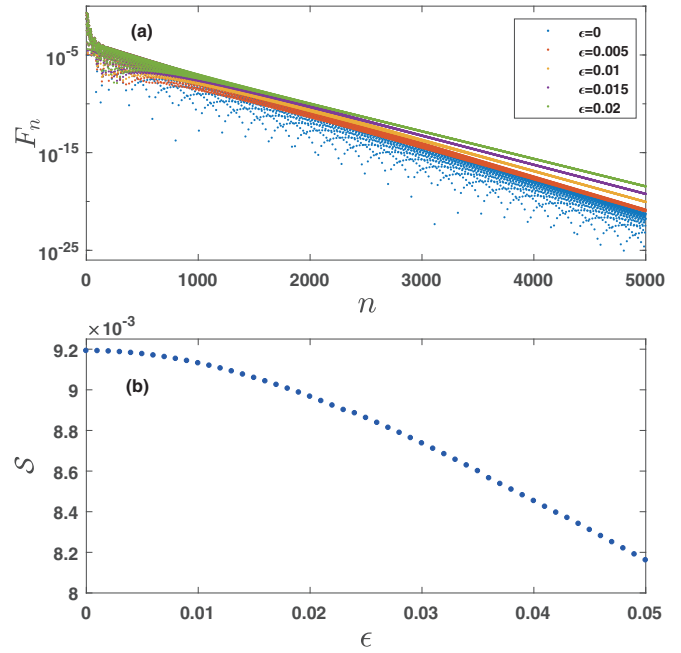


FIG. 6. F_n vs n for a sequentially perturbed system, and its decay rate S vs ϵ . $m = \frac{N}{2}$ perturbations are sequentially arranged on the ring system with $N = 22$ sites. The sample period is set at $\tau = 1$, and the initial position is set at $x_{in} = 0$. (a) Curves of F_n vs n when the perturbation strength ϵ varies from 0 to 0.02 with an interval of 0.005. (b) The relation between the slope of the asymptotic line and the perturbation strength.

their corresponding eigenvalues are $E_{k1} = 1.01258$ and $E_{l1} = -0.987578$, respectively. It can be found that both of the two eigenvectors have two zero entries. When $x_{in} = 0$ or 3, we do not break the reflection symmetry of the system, and the overlaps p_{k1} and p_{l1} equal zero, which leads to $\langle n \rangle = 4$. Similarly, in the periodically perturbed system, due to the overlaps being zero, $\langle n \rangle$ always equals $\frac{N}{2} + 1$ when the symmetry is preserved.

Apparently, compared with the unperturbed system, the perturbed system will generate an extra term including ϵ in all p_k terms. Hence ϵ can affect p_k and further influence the amplitude ϕ_n in Eq. (47).

2. The decay rate of F_n

The detection probability F_n is the square of the absolute value of the amplitude ϕ_n ; thus F_n is affected by ϵ . We

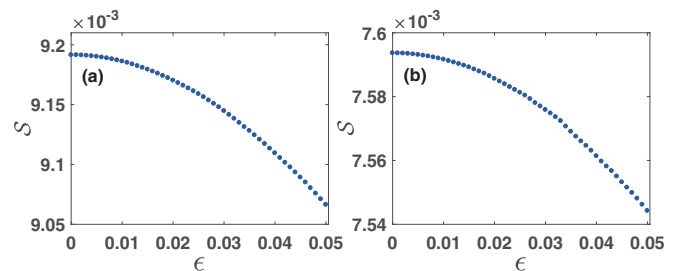


FIG. 7. The decay rate S vs ϵ . In the periodic perturbed system, the variables are set as $a = \frac{N}{2}$, $\tau = 1$, and $x_{in} = 0$. (a) Curve for $N = 22$, and (b) curve for $N = 24$.

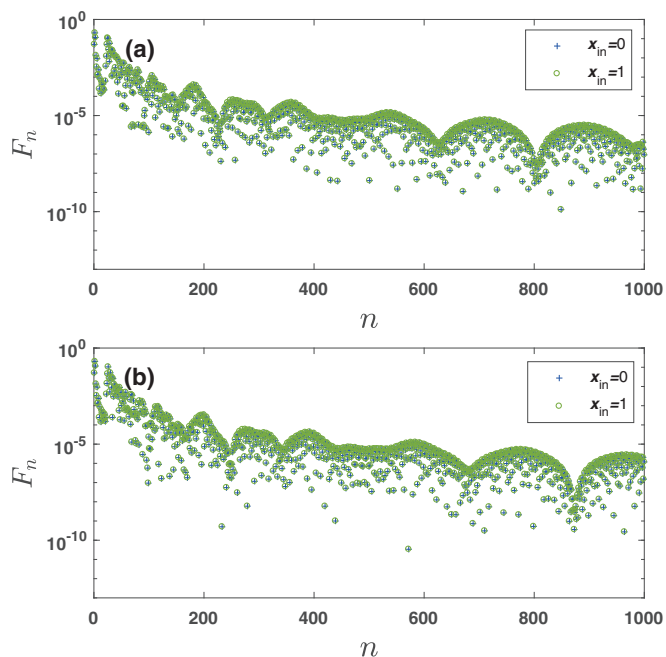


FIG. 8. F_n vs n for the periodically perturbed ring systems with $a = 2$. (a) For $N = 48$ and (b) for $N = 50$. The curves delineated with pluses and open circles show the results for $x_{in} = 0$ and 1, respectively.

demonstrate F_n in a ring system with sequentially arranged perturbations in Fig. 6. We set the sample period $\tau = 1$ and initial position $x_{in} = 0$. Figure 6(a) shows the curves when the amplitude of perturbations ϵ varies from 0 to 0.02 with an interval of 0.005. Apparently, the case of $\epsilon = 0$ means no

perturbation added. We can find that the decay rate \mathcal{S} , i.e., the slope of the asymptotic line, of the perturbed system is lower than that of the unperturbed system. The detailed result about the decay rate of detection probability F_n versus the amplitude of perturbations ϵ is shown in Fig. 6(b). The result shows that the decay rate \mathcal{S} is sensitive to the amplitude of perturbations ϵ , and the decay rate decreases with the increase in ϵ monotonically.

A similar relationship between decay rate \mathcal{S} and ϵ appears in the system with the periodic perturbation arrangement. The corresponding results are shown in Fig. 7. For simplicity, we set the interval equal to a half of the total site number, i.e., $a = \frac{N}{2}$. Figures 7(a) and 7(b) show the results for $\frac{N}{2}$ being odd and even, respectively. We can find that no matter whether $\frac{N}{2}$ is odd or even, the decay rate of the first detection probability F_n decreases with the increase in ϵ monotonically.

3. The coincidence of F_n

In the periodically perturbed system, F_n can display plentiful results. As the simplest periodic arrangement, the arrangement of perturbations with $a = 2$ cannot break the translation invariance of the perturbed ring system. So, different initial positions x_{in} will not change F_n . Figure 8 shows the curves of F_n versus n with $\epsilon = 0.05$. The ring sizes are set at $N = 48$ in Fig. 8(a) and $N = 50$ in Fig. 8(b). The curves delineated with pluses and open circles show the results for $x_{in} = 0$ and 1, respectively. The curves show that, no matter whether $\frac{N}{2}$ is even or odd, the curves of F_n are basically coincident for arbitrary initial position x_{in} .

However, $a = 2$ is not necessary to keep the curves of F_n coincident for different initial positions. In order to show this, we present F_n in Fig. 9 for different x_{in} in the periodically

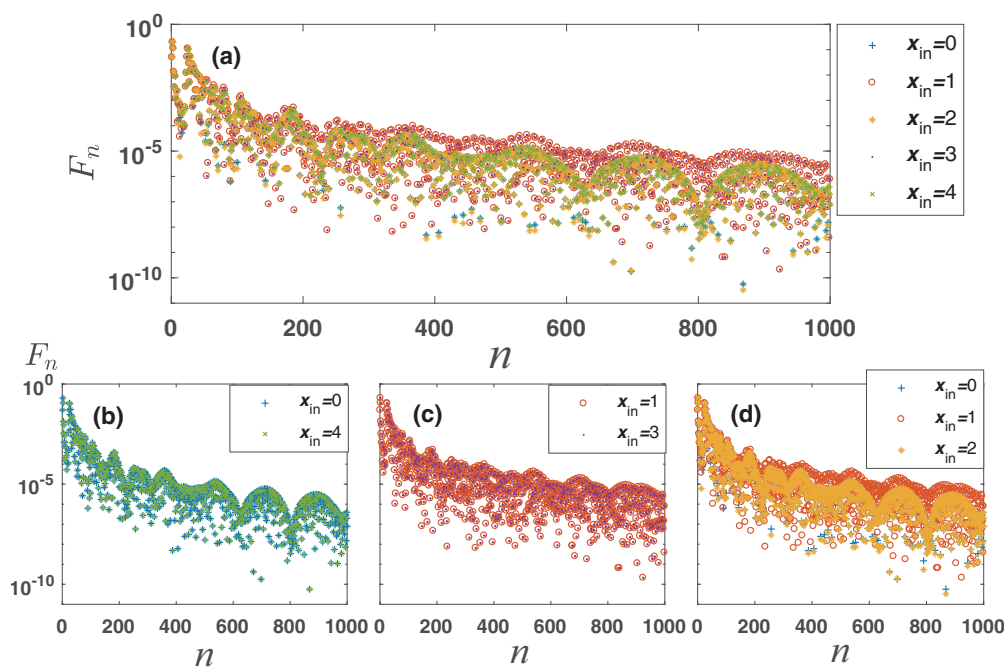


FIG. 9. F_n vs n for the periodically perturbed ring systems with $a = 4$. (a) The curves for the cases of $x_{in} = 0-4$, when $N = 48$ and $\epsilon = 0.05$. (b) The curves for $x_{in} = 0$ and 4. (c) The curves for $x_{in} = 1$ and 3. (d) The curves for $x_{in} = 0, 1$, and 2. (b) and (c) show the coincidence of F_n , and (d) shows the noncoincidence of F_n .

perturbed ring system with total sites $N = 48$, perturbation amplitude $\epsilon = 0.05$, and the interval $a = 4$. The curves for the cases of $x_{\text{in}} = 0-4$ are shown in Fig. 9(a). In order to better illustrate, we pick up the curve delineated with pluses ($x_{\text{in}} = 0$) and the curve delineated with crosses ($x_{\text{in}} = 4$) in Fig. 9(a) and list them in Fig. 9(b). We can find that the two curves are essentially coincident. The coincidence also appears in Fig. 9(c) for the cases of $x_{\text{in}} = 1$ (curve delineated with open circles) and $x_{\text{in}} = 3$ (curve delineated by dots). However, when $x_{\text{in}} = 0, 1$, and 2 , the corresponding curves of F_n are not coincident completely, as shown in Fig. 9(d). These results confirm that equal Δx for different initial positions leads to the coincidence of F_n curves. Hence, to a certain extent, the coincidence reflects the symmetry of the perturbed system.

IV. SUMMARY

In this paper, we studied the quantum first detection times in the perturbed ring systems. With time-independent perturbation theory, we obtained the general form of the eigenvalues and eigenvectors of the Hamiltonian and then discussed the perturbed systems with different spatial distributions in detail.

For the systems with sequential arrangements of perturbations, when the perturbed sites occupy half of the system, we find that in the leading order of the perturbation strength, all the energy levels increase by the same amount, although the numerical exact results show the split of energy levels. When the initial condition breaks the reflection symmetry of the system, the “weak” splitting of energy levels leads to novel behaviors of the finite sum, $\sum_{n=1}^{\mathcal{N}} nF_n$, that exhibits steplike growth as \mathcal{N} increases. We observe at least two plateaus pointing to the value of $\langle n \rangle$ in unperturbed systems and the size of the ring system, with the latter as the convergence of $\sum_{n=1}^{\mathcal{N}} nF_n$ when \mathcal{N} goes to infinity, namely, the exact $\langle n \rangle$ is equal to the size of the system. When the initial condition preserves the reflection symmetry, the mean return time is the same as the unperturbed system. For the systems with periodic arrangements of perturbations, the results of $\langle n \rangle$ are diverse. For the case of both $a = 2$ and $\frac{N}{2}$ being odd, all degeneracy of energy levels is not removed, and $\langle n \rangle$ is the same as the unperturbed system. For other cases, the degeneracy of energy levels is not completely maintained. The removal of degeneracy could lead to the increase in $\langle n \rangle$. Besides the removal of degeneracy, the initial positions can also influence the result of $\langle n \rangle$. The mean return time $\langle n \rangle$ has three possible results (see Table I); however, when the symmetry of the system is maintained, $\langle n \rangle$ chooses the smallest value $\frac{N}{2} + 1$. To summarize, in the study of the perturbed systems with different spatial distributions, we find that the distribution of perturbations ξ_j determines the removal of degeneracy [see Eq. (27)], and the choice of the initial condition determines whether the overlap p_k is nonzero. The mean return time $\langle n \rangle$ is equal to the amount of the nonzero overlaps w in Eq. (46), which means that $\langle n \rangle$ is less than or equal to N_E in Table I. Hence the choice of the perturbation site ξ_j and the initial condition affects the mean return time $\langle n \rangle$.

Moreover, in the study of the first detection probability F_n , we find that the decay rate \mathcal{S} of F_n is affected by perturbation amplitude ϵ . The decay rate \mathcal{S} decreases with the increase in perturbation amplitude ϵ (see Figs. 6 and 7). Furthermore, in

a periodically perturbed system, when the initial positions are equivalent, i.e., with the same Δx , the curves of F_n versus n coincide (see Figs. 8 and 9), and the values of $\langle n \rangle$ are equal.

In a finite system, if the degeneracy of the system is removed by the presence of perturbations, which means that the number of energy levels increases, both the mean return time $\langle n \rangle$ and the exceptional sampling time τ_c for different initial positions will be different, except for the equivalent initial positions. The fastest detection, the minimal value of $\langle n \rangle$, can be achieved only when the initial position does not break the reflection symmetry of the system. However, we can manipulate the spatial distribution of the perturbations to maintain degeneracy, so that the mean return time is the same as that in the unperturbed system to achieve the fastest detection.

ACKNOWLEDGMENTS

This work is supported by the National Natural Science Foundation of China (Grant No. 12104045). R.-Y.Y. is supported by Israel Science Foundation Grant No. 1614/21. Helpful discussions with E. Barkai are acknowledged.

APPENDIX A: CALCULATION OF EIGENVALUES AND EIGENVECTORS

Here we calculate the approximate results of eigenvalues and the corresponding eigenvectors. For the nondegenerate energy levels, the approximate results of eigenvalues and the corresponding eigenvectors are accurate to the second-order correction. According to Eq. (22), we have $E_0^{(1)} = E_{\frac{N}{2}}^{(1)} = -\epsilon \frac{m}{N}$. In order to get the results of $|E_0^{(1)}\rangle$ and $|E_{\frac{N}{2}}^{(1)}\rangle$, we substitute Eqs. (18)–(21) into Eq. (23), and straightforward calculation yields

$$|E_0^{(1)}\rangle = \frac{\epsilon}{2N\sqrt{N}} \sum_{n \neq 0}^m \sum_{j=1}^{N-1} \sum_{x=0}^{N-1} g_n \frac{\cos \frac{2\pi n(x-\xi_j)}{N}}{1 - \cos \frac{2\pi n}{N}} |x\rangle, \quad (\text{A1})$$

$$|E_{\frac{N}{2}}^{(1)}\rangle = \frac{\epsilon}{2N\sqrt{N}} \sum_{n \neq \frac{N}{2}}^m \sum_{j=1}^{N-1} \sum_{x=0}^{N-1} g_n \frac{(-1)^{\xi_j} \cos \frac{2\pi n(x-\xi_j)}{N}}{-1 - \cos \frac{2\pi n}{N}} |x\rangle. \quad (\text{A2})$$

Considering $|H'_{ni,l}|^2 \sim \epsilon^2$, we have $E_l^{(2)} \rightarrow 0$ in Eq. (24). Because of $H'_{mi,nj}, H'_{nj,l}, H'_{mi,l}, H'_{l,l} \sim \epsilon$, we have $\langle x | E_l^{(2)} \rangle \sim \epsilon^2$, and we can consider $|E_l^{(2)}\rangle$ in Eq. (25) as a zero vector. Hence, up to the second-order correction, we can write the nondegenerate energy levels $E_0, E_{\frac{N}{2}}$ and their eigenvectors as

$$E_0 = -2 - \epsilon \frac{m}{N}, \quad (\text{A3})$$

$$E_{\frac{N}{2}} = 2 - \epsilon \frac{m}{N}, \quad (\text{A4})$$

$$|E_0\rangle = \frac{\epsilon}{2N\sqrt{N}} \sum_{n \neq 0}^m \sum_{j=1}^{N-1} \sum_{x=0}^{N-1} \left[g_n \frac{\cos \left[\frac{2\pi n}{N} (x - \xi_j) \right]}{1 - \cos \frac{2\pi n}{N}} + \frac{2N}{\epsilon} \right] |x\rangle, \quad (\text{A5})$$

$$|E_{\frac{N}{2}}\rangle = \frac{\epsilon}{2N\sqrt{N}} \sum_{n \neq \frac{N}{2}}^m \sum_{j=1}^{N-1} \sum_{x=0}^{N-1} \left[g_n \frac{(-1)^{\xi_j} \cos \left[\frac{2\pi n}{N} (x - \xi_j) \right]}{-1 - \cos \frac{2\pi n}{N}} + (-1)^x \frac{2N}{\epsilon} \right] |x\rangle. \tag{A6}$$

For the degenerate energy levels, the approximate results of eigenvalues and the corresponding eigenvectors are accurate to the first-order correction. When the degeneracy is removed, we have $E_{l1}^{(1)} = -\frac{\epsilon}{N} (m - |\sum_{j=1}^m e^{i\frac{4\pi\xi_j l}{N}}|)$ and $E_{l2}^{(1)} = -\frac{\epsilon}{N} (m + |\sum_{j=1}^m e^{i\frac{4\pi\xi_j l}{N}}|)$, and we obtain the new zero-order eigenvectors for energy level $E_{l\alpha}^{(0)}$ in Eq. (28) as

$$|E_{l1}^{(0)}\rangle = \frac{1}{\sqrt{2N}} \sum_{x=0}^{N-1} (-e^{i\beta} e^{i\frac{2\pi l}{N}x} + e^{-i\frac{2\pi l}{N}x}) |x\rangle, \tag{A7}$$

$$|E_{l2}^{(0)}\rangle = \frac{1}{\sqrt{2N}} \sum_{x=0}^{N-1} (e^{i\beta} e^{i\frac{2\pi l}{N}x} + e^{-i\frac{2\pi l}{N}x}) |x\rangle. \tag{A8}$$

According to Eq. (30), the first-order correction of eigenvectors can be written in detail as

$$|E_{l1}^{(1)}\rangle = \frac{\epsilon}{(2N)^{\frac{3}{2}}} \sum_{n \neq l} \sum_{x=1}^{N-1} \sum_{j=1}^m \left\{ g_n (-e^{i\beta} e^{i\frac{2\pi\xi_j l}{N}} + e^{-i\frac{2\pi\xi_j l}{N}}) \times \frac{\cos \left[\frac{2\pi n}{N} (x - \xi_j) \right]}{\cos \frac{2\pi l}{N} - \cos \frac{2\pi n}{N}} \right\} |x\rangle, \tag{A9}$$

$$|E_{l2}^{(1)}\rangle = \frac{\epsilon}{(2N)^{\frac{3}{2}}} \sum_{n \neq l} \sum_{x=1}^{N-1} \sum_{j=1}^m \left\{ g_n (e^{i\beta} e^{i\frac{2\pi\xi_j l}{N}} + e^{-i\frac{2\pi\xi_j l}{N}}) \times \frac{\cos \left[\frac{2\pi n}{N} (x - \xi_j) \right]}{\cos \frac{2\pi l}{N} - \cos \frac{2\pi n}{N}} \right\} |x\rangle. \tag{A10}$$

Hence, when the degeneracy is removed in the first-order correction, the doubly degenerate energy level E_l splits into energy levels E_{l1} and E_{l2} . In the first-order correction, E_{l1} and E_{l2} are written as

$$E_{l1} = - \left[2 \cos \frac{2\pi l}{N} + \frac{\epsilon}{N} \left(m - \left| \sum_{j=1}^m e^{i\frac{4\pi l}{N} \xi_j} \right| \right) \right], \tag{A11}$$

$$E_{l2} = - \left[2 \cos \frac{2\pi l}{N} + \frac{\epsilon}{N} \left(m + \left| \sum_{j=1}^m e^{i\frac{4\pi l}{N} \xi_j} \right| \right) \right], \tag{A12}$$

respectively. Their corresponding eigenvectors are expressed as

$$|E_{l1}\rangle = \frac{\epsilon}{(2N)^{\frac{3}{2}}} \sum_{n \neq l} \sum_{x=1}^{N-1} \sum_{j=1}^m \left\{ \frac{2N}{\epsilon} [-e^{i(\frac{2\pi l}{N}x + \beta)} + e^{-i\frac{2\pi l}{N}x}] + \frac{g_n [-e^{i(\frac{2\pi\xi_j l}{N} + \beta)} + e^{-i\frac{2\pi\xi_j l}{N}}] \cos \frac{2\pi n(x - \xi_j)}{N}}{\cos \frac{2\pi l}{N} - \cos \frac{2\pi n}{N}} \right\} |x\rangle, \tag{A13}$$

$$|E_{l2}\rangle = \frac{\epsilon}{(2N)^{\frac{3}{2}}} \sum_{n \neq l} \sum_{x=1}^{N-1} \sum_{j=1}^m \left\{ \frac{2N}{\epsilon} [e^{i(\frac{2\pi l}{N}x + \beta)} + e^{-i\frac{2\pi l}{N}x}] + \frac{g_n [e^{i(\frac{2\pi\xi_j l}{N} + \beta)} + e^{-i\frac{2\pi\xi_j l}{N}}] \cos \frac{2\pi n(x - \xi_j)}{N}}{\cos \frac{2\pi l}{N} - \cos \frac{2\pi n}{N}} \right\} |x\rangle, \tag{A14}$$

respectively.

However, when the degeneracy is removed in the second-order correction but not in the first-order correction, namely, $E_{l1} = E_{l2} = -(2 \cos \frac{2\pi l}{N} + \frac{\epsilon}{N})$, using Eq. (28), we obtain the new zero-order eigenvectors as

$$|E_{l1}^{(0)}\rangle = \frac{1}{\sqrt{2N}} \sum_{x=0}^{N-1} (-e^{i\gamma} e^{i\frac{2\pi l}{N}x} + e^{-i\frac{2\pi l}{N}x}) |x\rangle, \tag{A15}$$

$$|E_{l2}^{(0)}\rangle = \frac{1}{\sqrt{2N}} \sum_{x=0}^{N-1} (e^{i\gamma} e^{i\frac{2\pi l}{N}x} + e^{-i\frac{2\pi l}{N}x}) |x\rangle. \tag{A16}$$

They are similar to Eqs. (A7) and (A8). Upon substituting Eqs. (A15) and (A16) into Eq. (30), we can obtain the first-order correction of eigenvectors

$$|E_{l1}^{(1)}\rangle = \frac{\epsilon}{(2N)^{\frac{3}{2}}} \sum_{n \neq l} \sum_{x=1}^{N-1} \sum_{j=1}^m \left\{ g_n (-e^{i\gamma} e^{i\frac{2\pi\xi_j l}{N}} + e^{-i\frac{2\pi\xi_j l}{N}}) \times \frac{\cos \left[\frac{2\pi n}{N} (x - \xi_j) \right]}{\cos \frac{2\pi l}{N} - \cos \frac{2\pi n}{N}} \right\} |x\rangle, \tag{A17}$$

$$|E_{l2}^{(1)}\rangle = \frac{\epsilon}{(2N)^{\frac{3}{2}}} \sum_{n \neq l} \sum_{x=1}^{N-1} \sum_{j=1}^m \left\{ g_n (e^{i\gamma} e^{i\frac{2\pi\xi_j l}{N}} + e^{-i\frac{2\pi\xi_j l}{N}}) \times \frac{\cos \left[\frac{2\pi n}{N} (x - \xi_j) \right]}{\cos \frac{2\pi l}{N} - \cos \frac{2\pi n}{N}} \right\} |x\rangle. \tag{A18}$$

Hence the corresponding eigenvectors in the first-order correction are expressed as

$$|E_{l1}\rangle = \frac{\epsilon}{(2N)^{\frac{3}{2}}} \sum_{n \neq l} \sum_{x=1}^{N-1} \sum_{j=1}^m \left\{ \frac{2N}{\epsilon} [-e^{i(\frac{2\pi l}{N}x + \gamma)} + e^{-i\frac{2\pi l}{N}x}] + \frac{g_n [-e^{i(\frac{2\pi\xi_j l}{N} + \gamma)} + e^{-i\frac{2\pi\xi_j l}{N}}] \cos \left[\frac{2\pi n}{N} (x - \xi_j) \right]}{\cos \frac{2\pi l}{N} - \cos \frac{2\pi n}{N}} \right\} |x\rangle, \tag{A19}$$

$$|E_{l2}\rangle = \frac{\epsilon}{(2N)^{\frac{3}{2}}} \sum_{n \neq l} \sum_{x=1}^{N-1} \sum_{j=1}^m \left\{ \frac{2N}{\epsilon} [e^{i(\frac{2\pi l}{N}x + \gamma)} + e^{-i\frac{2\pi l}{N}x}] + \frac{g_n [e^{i(\frac{2\pi\xi_j l}{N} + \gamma)} + e^{-i\frac{2\pi\xi_j l}{N}}] \cos \left[\frac{2\pi n}{N} (x - \xi_j) \right]}{\cos \frac{2\pi l}{N} - \cos \frac{2\pi n}{N}} \right\} |x\rangle, \tag{A20}$$

respectively.

APPENDIX B: DERIVATION OF TABLE I

Here we derive the relation between the size of the ring N , the interval a , the initial position x_{in} , and the mean return time $\langle n \rangle$ for the systems with periodic arrangements of perturbations. When $\frac{2la}{N}$ is an integer, we have $e^{i\frac{4\pi l}{N}a} = 1$ and Eq. (38). According to Eq. (36), the corresponding degenerate energy level splits. Using Eq. (38), we obtain

$$e^{i\beta} = \frac{\sum_{j=1}^m e^{-i\frac{4\pi l}{N}aj}}{\left| \sum_{j=1}^m e^{i\frac{4\pi l}{N}aj} \right|} = 1. \tag{B1}$$

Upon substituting Eq. (B1) into Eqs. (A13) and (A14), we get the corresponding eigenvectors in the periodically perturbed systems

$$|E_{l1}\rangle = \frac{-i\epsilon}{\sqrt{2N^{\frac{3}{2}}}} \sum_{n \neq l} \sum_{x=1}^{N-1} \sum_{j=1}^m \left[\frac{2N}{\epsilon} \sin \frac{2\pi lx}{N} + g_n \frac{\cos \frac{2\pi n(x-\xi_j)}{N} \sin \frac{2\pi \xi_j l}{N}}{\cos \frac{2\pi l}{N} - \cos \frac{2\pi n}{N}} \right] |x\rangle, \tag{B2}$$

$$|E_{l2}\rangle = \frac{\epsilon}{\sqrt{2N^{\frac{3}{2}}}} \sum_{n \neq l} \sum_{x=1}^{N-1} \sum_{j=1}^m \left[\frac{2N}{\epsilon} \cos \frac{2\pi lx}{N} + g_n \frac{\cos \frac{2\pi n(x-\xi_j)}{N} \cos \frac{2\pi \xi_j l}{N}}{\cos \frac{2\pi l}{N} - \cos \frac{2\pi n}{N}} \right] |x\rangle. \tag{B3}$$

The mean return time $\langle n \rangle$ in the return problem depends on the effective dimension of the underlying Hilbert space, which is given by the number of distinct energy phases $\exp(iE_l\tau)$ with nonzero overlaps between the corresponding eigenvectors and the target state. We calculate the overlap $\langle x_d | E_{l\alpha} \rangle$ to determine the mean return time $\langle n \rangle$ in arbitrary target states.

In the case of the degenerate energy levels splitting, $\frac{2la}{N}$ is an integer, i.e., $l = \kappa_1 \frac{N}{2a}$, where κ_1 is a non-negative integer and $0 < \kappa_1 < a$. It can be found that the second term in the square brackets in Eq. (B2) is identically vanishing. We can simplify Eq. (B2) into

$$|E_{l1}\rangle = -i\sqrt{\frac{2}{N}} \sum_{x=1}^{N-1} \sin \frac{2\pi lx}{N} |x\rangle. \tag{B4}$$

When the overlap $\langle x | E_{l1} \rangle = 0$, i.e., $\frac{2\pi lx}{N} = \kappa_2\pi$, the position $x = \kappa_2 \frac{N}{2l} = \kappa_2 \frac{a}{\kappa_1}$, where $x = 0, 1, \dots, N-1$ and κ_2 is a non-negative integer. For the case of even a , x equals a multiple of $\frac{a}{2}$ or a multiple of b_i , where b_i is a divisor of a and $1 < b_i < \frac{a}{2}$. For the case of odd a , when a is a composite number, x equals a multiple of a or a multiple of b_i ; otherwise (a is a prime number), x just equals a multiple of a . According to Eq. (B4), for the case of x being a multiple of $\frac{a}{2}$ or just a multiple of a , we have the overlap $\langle x | E_{l1} \rangle = 0$ in all eigenvectors $|E_{l1}\rangle$. For other cases, when a is a composite number and $a = b_i \times c_i$, where $1 < c_i < a$, we have the overlap $\langle x | E_{l1} \rangle = 0$ under the conditions of κ_1 being a multiple of c_i and x being a multiple

of b_i . Apparently, the number of κ_1 is $b_i - 1$. Hence, when x is a multiple of b_i , we have the overlap $\langle x | E_{l1} \rangle = 0$ in $b_i - 1$ eigenvectors $|E_{l1}\rangle$.

We then discuss the overlap $\langle x | E_{l2} \rangle$. For the first term in the square brackets in Eq. (B3), when $\cos \frac{2\pi lx}{N} = 0$, i.e., $\frac{2\pi lx}{N} = (\kappa_2 + \frac{1}{2})\pi$, we get $x = (\kappa_2 + \frac{1}{2})\frac{N}{2l} = \frac{(2\kappa_2+1)a}{2\kappa_1}$. Only if the interval a is even do there exist solutions of x , and x equals an odd multiple of $\frac{a}{2}$. Hence, when the overlap $\langle x | E_{l2} \rangle = 0$, a must be even.

For the second term in the square brackets in Eq. (B3), we obtain $\cos \frac{2\pi \xi_j l}{N} = (-1)^{\kappa_1 j}$, i.e., $\frac{2\pi \xi_j l}{N} = \frac{2al}{N} j\pi = \kappa_1 j\pi$. Hence the second term in the square brackets in Eq. (B3) can be rewritten as

$$g_n \frac{\cos \frac{2\pi n(x-\xi_j)}{N} \cos \frac{2\pi \xi_j l}{N}}{\cos \frac{2\pi l}{N} - \cos \frac{2\pi n}{N}} = g_n \frac{\cos \frac{2\pi n(x-\xi_j)}{N} (-1)^{\kappa_1 j}}{\cos \frac{2\pi l}{N} - \cos \frac{2\pi n}{N}}. \tag{B5}$$

According to the relation between trig functions and complex exponentials, we obtain the summation

$$\begin{aligned} & \sum_{j=1}^m \cos \frac{2\pi n(x-\xi_j)}{N} (-1)^{\kappa_1 j} \\ &= \frac{1}{2} \left[e^{i\frac{2\pi nx}{N}} \sum_{j=1}^m e^{i(\kappa_1 - \frac{2na}{N})j\pi} + e^{-i\frac{2\pi nx}{N}} \sum_{j=1}^m e^{-i(\kappa_1 - \frac{2na}{N})j\pi} \right]. \end{aligned} \tag{B6}$$

For the general case, i.e., $e^{i(\kappa_1 - \frac{2na}{N})j\pi} \neq 1$, Eq. (B6) takes the simple form

$$\begin{aligned} & \sum_{j=1}^m \cos \frac{2\pi n(x-\xi_j)}{N} (-1)^{\kappa_1 j} \\ &= \cos \left[\frac{\kappa_1(m-1)}{2} + \frac{n(2x+a)}{N} - n \right] \frac{\sin \left(\frac{\kappa_1 m}{2} - n \right) \pi}{\sin \left(\frac{\kappa_1}{2} - \frac{n}{N} a \right) \pi}. \end{aligned} \tag{B7}$$

Because $l (= \kappa_1 \frac{N}{2a} = \kappa_1 \frac{m}{2})$ is an integer, if κ_1 is odd, the number of perturbations m must be even. Then, the value of Eq. (B7) is equal to zero. However, when $\kappa_1 - \frac{2na}{N}$ is even, we get $\sum_{j=1}^m e^{i(\kappa_1 - \frac{2na}{N})j\pi} = \sum_{j=1}^m e^{-i(\kappa_1 - \frac{2na}{N})j\pi} = m$, and the value of Eq. (B6) is nonzero.

To sum up, if the overlap $\langle x | E_{l2} \rangle = 0$, four conditions must be satisfied simultaneously: The interval a is even, x equals an odd multiple of $\frac{a}{2}$, the number of perturbations m is even, and κ_1 is odd. Apparently, when $\frac{N}{2}$ is odd, a and m cannot be even simultaneously. When $\frac{N}{2}$ and a are even, κ_1 is odd, and x equals odd multiples of $\frac{a}{2}$, we have the overlap $\langle x | E_{l2} \rangle = 0$. In addition, when the energy levels are nondegenerate, and the degeneracy is not removed, we find that the overlaps are nonzero in Eqs. (18), (19), (A19), and (A20). Finally, we summarize the above results and obtain Table I based on the relation between the number of distinct energy phases $\exp(iE_l\tau)$ with nonzero overlaps and the mean return time $\langle n \rangle$.

[1] S. Redner, *A Guide to First-Passage Processes*, 1st ed. (Cambridge University Press, Cambridge, 2001).

[2] H. W. McKenzie, M. A. Lewis, and E. H. Merrill, First passage time analysis of animal movement and insights

- into the functional response, *Bull. Math. Biol.* **71**, 107 (2009).
- [3] M. L. Mayo, E. J. Perkins, and P. Ghosh, First-passage time analysis of a one-dimensional diffusion-reaction model: application to protein transport along DNA, *BMC Bioinf.* **12**, S18 (2011).
- [4] A. J. Bray, S. N. Majumdar, and G. Schehr, Persistence and first-passage properties in nonequilibrium systems, *Adv. Phys.* **62**, 225 (2013).
- [5] O. Bénichou, T. Guérin, and R. Voituriez, Mean first-passage times in confined media: from Markovian to non-Markovian processes, *J. Phys. A: Math. Theor.* **48**, 163001 (2015).
- [6] A. Godec and R. Metzler, First passage time distribution in heterogeneity controlled kinetics: going beyond the mean first passage time, *Sci. Rep.* **6**, 20349 (2016).
- [7] H. Vanvinckenroye, T. Andrianne, and V. Denoël, First passage time as an analysis tool in experimental wind engineering, *J. Wind Eng. Ind. Aerodyn.* **177**, 366 (2018).
- [8] A. Kumar, A. Zodage, and M. S. Santhanam, First detection of threshold crossing events under intermittent sensing, *Phys. Rev. E* **104**, L052103 (2021).
- [9] S. Dhar, S. Dasgupta, and A. Dhar, Quantum time of arrival distribution in a simple lattice model, *J. Phys. A: Math. Theor.* **48**, 115304 (2015).
- [10] S. Dhar, S. Dasgupta, A. Dhar, and D. Sen, Detection of a quantum particle on a lattice under repeated projective measurements, *Phys. Rev. A* **91**, 062115 (2015).
- [11] F. A. Grünbaum, L. Velázquez, A. H. Werner, and R. F. Werner, Recurrence for discrete time unitary evolutions, *Commun. Math. Phys.* **320**, 543 (2013).
- [12] J. Bourgain, F. A. Grünbaum, L. Velázquez, and J. Wilkening, Quantum recurrence of a subspace and operator-valued Schur functions, *Commun. Math. Phys.* **329**, 1031 (2014).
- [13] H. Krovi and T. A. Brun, Hitting time for quantum walks on the hypercube, *Phys. Rev. A* **73**, 032341 (2006).
- [14] H. Krovi and T. A. Brun, Quantum walks with infinite hitting times, *Phys. Rev. A* **74**, 042334 (2006).
- [15] H. Krovi and T. A. Brun, Quantum walks on quotient graphs, *Phys. Rev. A* **75**, 062332 (2007).
- [16] M. Varbanov, H. Krovi, and T. A. Brun, Hitting time for the continuous quantum walk, *Phys. Rev. A* **78**, 022324 (2008).
- [17] C. F. Chiang and G. Gomez, Hitting time of quantum walks with perturbation, *Quantum Inf. Process.* **12**, 217 (2013).
- [18] H. Friedman, D. A. Kessler, and E. Barkai, Quantum renewal equation for the first detection time of a quantum walk, *J. Phys. A: Math. Theor.* **50**, 04LT01 (2017).
- [19] H. Friedman, D. A. Kessler, and E. Barkai, Quantum walks: The first detected passage time problem, *Phys. Rev. E* **95**, 032141 (2017).
- [20] F. Thiel, E. Barkai, and D. A. Kessler, First Detected Arrival of a Quantum Walker on an Infinite Line, *Phys. Rev. Lett.* **120**, 040502 (2018).
- [21] R. Yin, K. Ziegler, F. Thiel, and E. Barkai, Large fluctuations of the first detected quantum return time, *Phys. Rev. Res.* **1**, 033086 (2019).
- [22] D. Meidan, E. Barkai, and D. A. Kessler, Running measurement protocol for the quantum first-detection problem, *J. Phys. A: Math. Theor.* **52**, 354001 (2019).
- [23] Q. Liu, R. Yin, K. Ziegler, and E. Barkai, Quantum walks: The mean first detected transition time, *Phys. Rev. Res.* **2**, 033113 (2020).
- [24] F. Thiel, D. A. Kessler, and E. Barkai, Quantization of the mean decay time for non-Hermitian quantum systems, *Phys. Rev. A* **102**, 022210 (2020).
- [25] D. A. Kessler, E. Barkai, and K. Ziegler, First-detection time of a quantum state under random probing, *Phys. Rev. A* **103**, 022222 (2021).
- [26] K. Ziegler, E. Barkai, and D. Kessler, Randomly repeated measurements on quantum systems: correlations and topological invariants of the quantum evolution, *J. Phys. A: Math. Theor.* **54**, 395302 (2021).
- [27] A. Didi and E. Barkai, Measurement-induced quantum walks, *Phys. Rev. E* **105**, 054108 (2022).
- [28] P. Sinkovicz, Z. Kurucz, T. Kiss, and J. K. Asbóth, Quantized recurrence time in unital iterated open quantum dynamics, *Phys. Rev. A* **91**, 042108 (2015).
- [29] P. Sinkovicz, T. Kiss, and J. K. Asbóth, Generalized Kac lemma for recurrence time in iterated open quantum systems, *Phys. Rev. A* **93**, 050101(R) (2016).
- [30] G. Pólya, Über eine Aufgabe der Wahrscheinlichkeitsrechnung betreffend die Irrfahrt im Strabennetz, *Math. Ann.* **84**, 149 (1921).
- [31] S. Tornow and K. Ziegler, Measurement induced quantum walks on an IBM quantum computer, [arXiv:2210.09941](https://arxiv.org/abs/2210.09941) [quant-ph].
- [32] F. Thiel, I. Mualem, D. Meidan, E. Barkai, and D. A. Kessler, Dark states of quantum search cause imperfect detection, *Phys. Rev. Res.* **2**, 043107 (2020).
- [33] P. Törmä, I. Jex, and W. P. Schleich, Localization and diffusion in Ising-type quantum networks, *Phys. Rev. A* **65**, 052110 (2002).
- [34] N. V. Prokof'ev and P. C. E. Stamp, Decoherence and quantum walks: Anomalous diffusion and ballistic tails, *Phys. Rev. A* **74**, 020102(R) (2006).
- [35] Y. Yin, D. E. Katsanos, and S. N. Evangelou, Quantum walks on a random environment, *Phys. Rev. A* **77**, 022302 (2008).
- [36] Z. J. Li, J. A. Izaac, and J. B. Wang, Position-defect-induced reflection, trapping, transmission, and resonance in quantum walks, *Phys. Rev. A* **87**, 012314 (2013).
- [37] A. Schreiber, K. N. Cassemiro, V. Potoček, A. Gábris, I. Jex, and Ch. Silberhorn, Decoherence and Disorder in Quantum Walks: From Ballistic Spread to Localization, *Phys. Rev. Lett.* **106**, 180403 (2011).
- [38] T. Xu and R. V. Krems, Quantum walk and Anderson localization of rotational excitations in disordered ensembles of polar molecules, *New J. Phys.* **17**, 065014 (2015).
- [39] P. W. Anderson, Absence of Diffusion in Certain Random Lattices, *Phys. Rev.* **109**, 1492 (1958).
- [40] J. P. Keating, N. Linden, J. C. F. Matthews, and A. Winter, Localization and its consequences for quantum walk algorithms and quantum communication, *Phys. Rev. A* **76**, 012315 (2007).
- [41] A. Joye and M. Merkli, Dynamical localization of quantum walks in random environments, *J. Stat. Phys.* **140**, 1025 (2010).
- [42] A. Wójcik, T. Łuczak, P. Kurzyński, A. Grudka, T. Gdala, and M. Bednarska-Bzdga, Trapping a particle of a quantum walk on the line, *Phys. Rev. A* **85**, 012329 (2012).

- [43] Y. Lahini, A. Avidan, F. Pozzi, M. Sorel, R. Morandotti, D. N. Christodoulides, and Y. Silberberg, Anderson Localization and Nonlinearity in One-Dimensional Disordered Photonic Lattices, *Phys. Rev. Lett.* **100**, 013906 (2008).
- [44] E. Agliari, O. Mülken, and A. Blumen, Continuous-time quantum walks and trapping, *Int. J. Bifurcation Chaos* **20**, 271 (2010).
- [45] G. Pozzoli and B. De Bruyne, Survival probability of random walks leaping over traps, *J. Stat. Mech.* **2021**, 123203 (2021).
- [46] L. I. Schiff, *Quantum Mechanics*, 2nd ed. (McGraw-Hill, New York, 1955).
- [47] F. L. H. Brown, Generating function methods in single-molecule spectroscopy, *Acc. Chem. Res.* **39**, 363 (2006).
- [48] C. Cohen-Tannoudji, B. Diu, and F. Laloë, *Quantum Mechanics* (Wiley, New York, 1977).